2. JT-60U Tokamak

2.1 Tokamak

In the early 1950s, the development of tokamaks at the Kurchatov Institute in the Soviet Union were followed by Tamm and Sakharov. The successful development of the tokamak was principally the result of the careful attention paid to the reduction of impurities and the separation of the plasma from the vacuum vessel by means of a 'limiter'. This led during the 1960s to comparatively pure plasmas with electron temperatures of around 1 keV [1]. By 1970 these results were generally accepted and their significance appreciated and many tokamaks were constructed in the world [2]. Tokamak research concentration has led to a large scale world wide program. In tokamak research, although the basic configuration of the tokamak has not relatively changed, the development of larger experiments with high power additional heating, improved plasma control, vessel conditioning techniques, mechanical support systems, magnetic divertor and diagnostic systems have progressed.

In the 1980s, three large tokamaks [3]: TFTR at the Princeton Plasma Laboratory, USA (however, programs finished in 1997); JET at the Culham Laboratories in the UK; JT-60U at Naka Fusion Research establishment in Japan, were constructed to satisfy the Lawson criterion. Up to the present, the JET and JT-60U achieved the break-even plasma condition, and TFTR and JET have performed the deuterium-tritium mixture discharges, then JET have successfully gained the fusion power up to 16MW in actual deuterium-tritium mixture discharges [4-7]. In light of importance of divertor physics in the design of next step devices, divertor geometry was modified in JET and JT-60U.

In 1982, the higher confinement regime, which showed about factor two improvement of confinement is discovered in auxiliary heated discharged on ASDEX in Germany. This is called the H-mode [8] in contrast with a normal regime called as the L-mode. The transition to that state was found in a plasma with a divertor configuration. The improvement was found mainly at the plasma edge. The H-mode produces steep

gradients of density and temperature in the edge region as shown in Fig.2.1, which is called Edge Transport Barrier (ETB), and by its steep gradients, instabilities so-called Edge Localized Mode (ELMs) are driven. These are rapid bursts of MHD activity accompanied by poor plasma confinement and producing large heat and particle fluxes to plasma-facing conponents. However, small frequent ELMs are considered to be desirable for steady-state tokamak operation as they expel impurities including helium ash and stabilize the core plasma density.

In 1998, high fusion performance has been obtained in low q_s, high I_p reversed shear discharges with Internal Transport Barrier (ITB) on JT-60U. ITB works as electron and ion thermal barrier and makes gradient or temperature and density very steep as shown in Fig.2.1. The ITB observed in JT-60U has an outstanding feature that electron and ion thermal diffusivities are simultaneously reduced with a steep temperature gradient around a thin ITB layer [9].

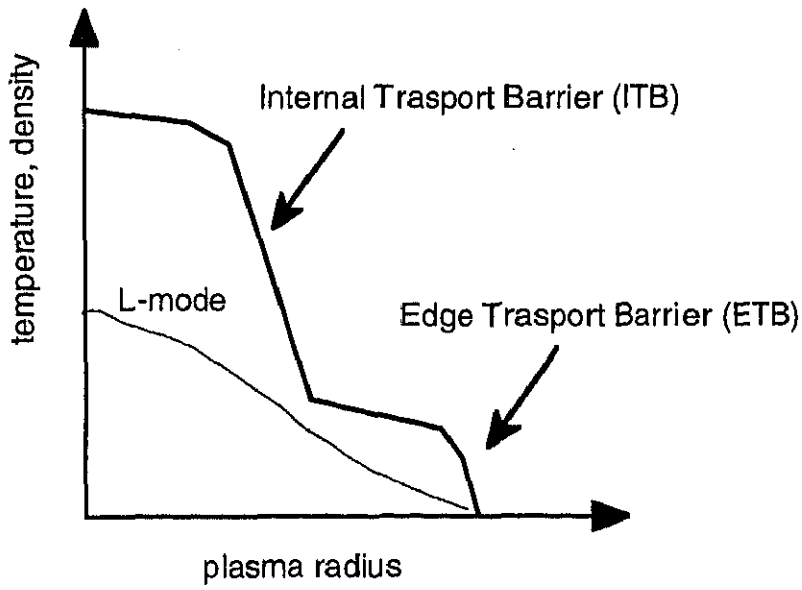

Figure 2.1 *Illustration for explanation of Internal Transport Barrier and Edge Transport Barrier*

2.1.1 Fundamental principle

The Tokamak is a toroial plasma confinement system, the plasma being confined by magnetic field [3]. The word 'tokamak' is derived from the Russian word acronym for "Toroidalnaya Kamera ee Magnitnaya Katushka", which means toroidal chamber and magnetic coil. The principle magnetic field is toroidal field. However, for plasma confinement, this toroidal field alone is not sufficient and poloidal magnetic field induced by currents flowing in the plasma itself is also required. The combination of the toroidal field and the poloidal field gives rise to magnetic filed lines which have a helical trajectory around the torus.

The geometry and coordinate system are shown in figure 2.2 and an example of a tokamak machine is shown in figure 2.3. The tokamak consists of toroidal vacuum vessel and several magnetic coils. The toroidal magnetic field B_ϕ is produced by the toroidal coils. The poloidal magnetic field B_θ is produced by a plasma current I_p which is driven by a toroidal electric field E induced by transformer action with the plasma acting as a single turn secondary.

The major radius R_0 is the distance from the toroidal axis. The two minor radii a and b are the horizontal and vertical distances from the magnetic axis to the edge of the plasma. The ratio R_0/a, characterizing the fatness of the torus, is the aspect ratio. The ratio b/a is elongation of the plasma cross section.

There are advantages for confinement and achievable pressure with higher plasma current by increasing vertically the elongation. The plasma shape, elongation, and the position of the plasma is controlled by the additional poloidal field coils. The spatial variation of the toroidal magnetic field strength is approximately given by;

$$B_\phi = \frac{B_0 R_0}{R}, \tag{2.1}$$

where B_0 is the magnetic field strength at the center of the plasma. In a uniform magnetic field, the changed particle has a spiral orbit composed of the circular motion and a constant velocity in the direction of the magnetic field. The circular orbit has a radius ρ_r

defined as

$$\rho_r = \frac{mv_\perp}{Z|e|B}, \tag{2.2}$$

where m is the mass, e is the electric charge, $v_\perp$ is the perpendicular velocity to the magnetic field, Z is the charged number of ion, Z = 1 for electron.

The principal for plasma confinement in a tokamak is to use the strong toroidal field and confine the charged particle along the magnetic field line. However, this toroidal field is not sufficient to confine a charged particle. When there is the gradient of magnetic field, the ρ_r has a different curvature on the part of its orbit in plasma. This leads to a drift perpendicular to both the magnetic field and its gradient. This drift is called ∇B drift. Moreover, when a particle's guiding center follows a curved magnetic field line, it undergoes a drift perpendicular to the plane in which the curvature lies. This drift is called curvature drift. In the case there is the toroidal field alone, curvature drift is in the same direction as the ∇B drift. A velocity caused by both the ∇B drift and the curvature drift is given by:

$$v_{dr} = -\frac{m}{qB_0R_0}\left(v_{//}^2 + \frac{v_\perp^2}{3}\right)e_z, \tag{2.3}$$

where $v_{//}$ is the parallel velocity along the magnetic field and e_z is the unit vector in the direction of the vertical axis. The ion moves toward the upper side of the torus and electron moves the lower side if the field B is counter clockwise viewing from the top of the torus. This leads to a charge separation and makes electric field **E**. The $\mathbf{E}\times\mathbf{B}$ drift by the charge separation throws out the plasma outward of the major radius. When there is the plasma current in toroidal direction, the force which expands the plasma current works the plasma. This is because the inside magnitude of the magnetic-flux density is larger than outside one. This outward force is called hoop force, this force is balanced by applying a vertical magnetic field which interacts with the toroidal current to give an inward force. The position control coil which makes vertical a magnetic field is installed

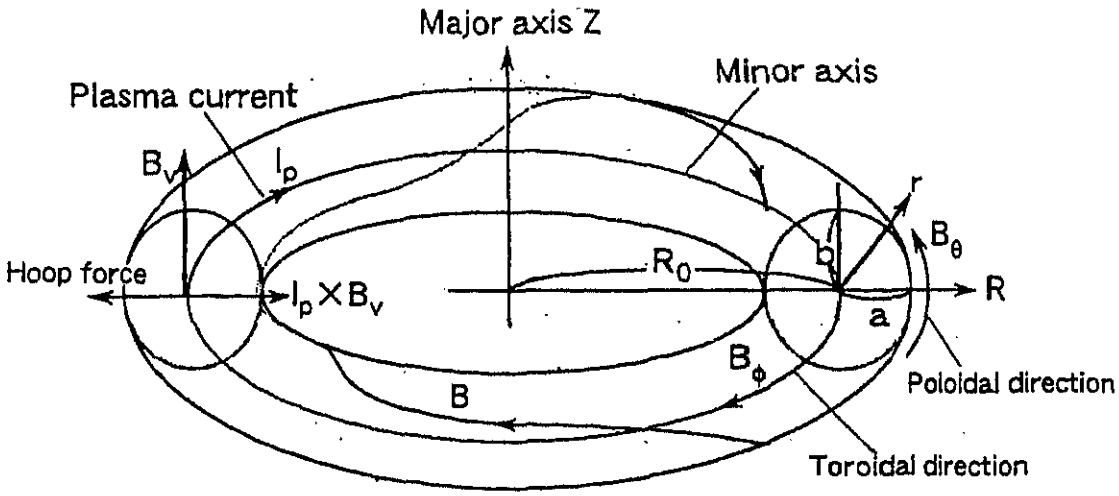

B_ϕ : Toroidal magnetic field
I_p : Plasma current
B_θ : Poloidal magnetic field
B_v : Vertical magnetic field
B : Magnetic field line
R_0 : Major radius
b : Minor radius (horizontal)
a : Minor radius (vertical)

Figure 2.2 *Toroidal geometry of the tokamak and coordinate system.*

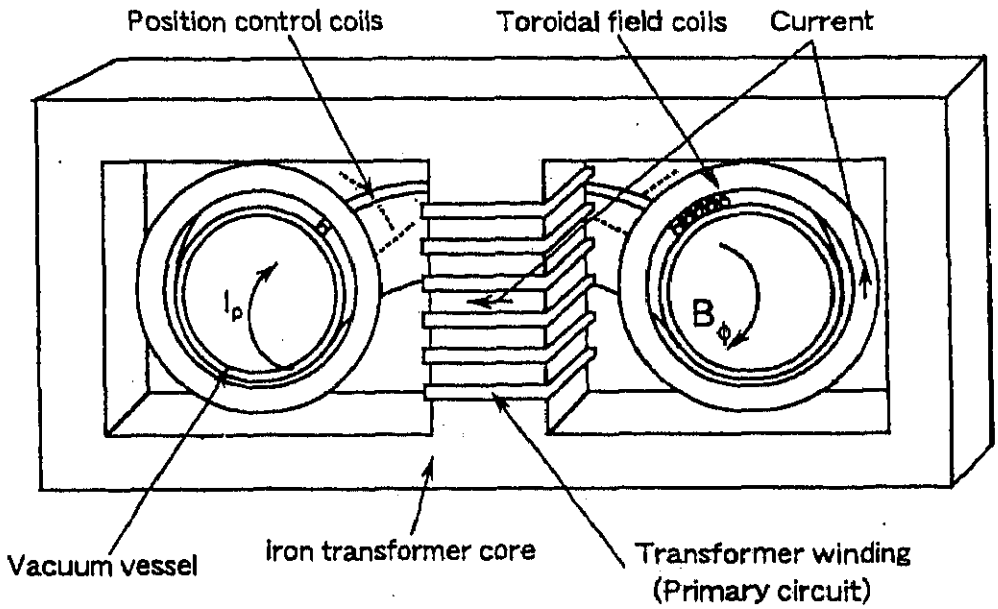

Figure 2.3 *Schematic of the Tokamak configuration*

to cancel the hoop force. The position control coil which makes a vertical magnetic field is installed to cancel the hoop force.

The pitch of the helical field line in the tokamak is characterized by the safety factor q_s. For a large aspect ratio plasma with a circular cross-section, the safety factor is written as

$$q_s(r) = \frac{r}{R_0}\frac{B_\phi}{B_\theta(r)}, \tag{2.5}$$

where r is the minor radius of the flux surface. The safety factor presents the number of complete toroidal turns of the field line before completing a single poloidal turn. It is a very important factor in determining overall stability of the plasma. The low-q discharges cause instabilities where poloidal magnetic field have the form $\exp i(m\theta - n\phi)$ where m and n being the poloidal and toroidal mode numbers, and these instabilities frequently lead to an abrupt quench of a plasma current, which is called Disruption. Consequently, the q_s profile emerges as a critical factor in determining the overall stability of tokamak plasmas. Other important factor in mageto-hydrodynamic (MHD) stability include the ratio of the plasma pressure to magnetic field pressure β.

2.1.2 Present tokamak configuration

Most present tokamak has a poloidal divertor configuration, which is beneficial to isolate the core plasma from plasma-wall interaction as illustrated in Fig.2.4. The divertor configuration is available to separate the main plasma from the first wall. In the divertor configuration, plasma is simply divided into four regions; confined region, scrape-off layer (SOL) region, private region, and divertor region. The boundary between the confined and SOL region is referred to as the last closed flux surface (LCFS) or the separatrix (which also includes the boundary between the private and the divertor).

The divertor configuration is produced by the additional divertor coil in the toroidal direction. Divertor coil current flows in the same direction as the plasma current. The poloidal magnetic field B_0 is null at the x-point. The shape of LCFS is also controlled by

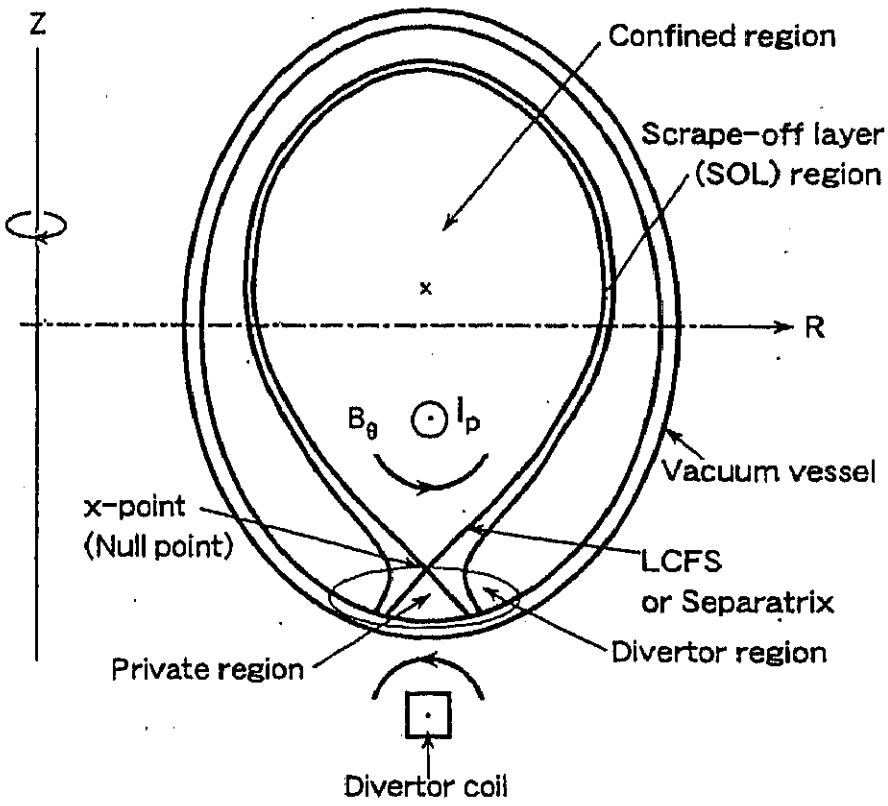

Figure2.4 *Tokamak configuration with the divertor. The divertor configuration is produced by the divertor coil with the current flowing to the same direction in the plasma current.*

external coils. The plasma particle and heat exhausted from the confined region are conducted to the divertor target along the SOL magnetic field line. The advantage of the divertor configuration is to reduce the neutral particles and impurities generated by plasma-wall interaction entering the main plasma. However, the small area in divertor target is compelled to receive large heat flux. In a fusion reactor the design of the divertor will be very important to control the power reaching the target surface.

2.2 JT-60U device

JT-60 [10, 11] is a large tokamak type experimental device which began its

operation from April 1985. The original JT-60 had a closed divertor chamber situated on the large major radius side of the plasma. But this configuration and lack of deuterium operation capability did not allow a high quality H-mode operation. To permit the H-mode operation and improve the plasma performance, JT-60 was modified to JT-60U (JT-60 Upgrade) which is capable of deuterium operation and high plasma current up 6MA with single null x-point at the bottom of the vacuum vessel between November 1988 and May 1991. The divertor of JT-60U was also modified from open divertor to a W-shaped divertor with pumps in 1997 [12]

An overall schematic view of the JT-60U is shown in Fig. 2.5. JT-60U has 18 toroidal field coils. The operational parameters of JT-60U are summarized in Table.2.1. JT-60U is capable of hydrogen, deuterium, and helium gas operation. The first wall is completely covered with graphite, especially with carbon fiber composite (CFC) tiles in the divertor target. Therefore, the dominant impurity in the plasma is carbon.

In JT-60U a variety of confinement regimes to be investigated can be allowed by several additional heating system as following

2.3 Additional heating system of JT-60U

The ohmic heating is induced by the resistance to the toroidal current caused by electron-ion collisions. The plasma is heated up to temperature of a few keV. The ohmic heating power decreases as the temperature increases with a $T_e^{-3/2}$ dependence of the plasma resistivity. To achieve a temperature higher than 10 keV, additional heating system such as neutral beam injection and radio-frequency heating are used. In the former, high energy neutral atoms are injected into the plasma so as to penetrate through the tokamak's magnetic field. In the latter, high power electromagnetic waves are injected into the plasma and heat the plasma through resonant interactions.

2.3.1 Neutral beam system

The neutral beam injection (NBI) of JT-60U is carried out by two type of injection

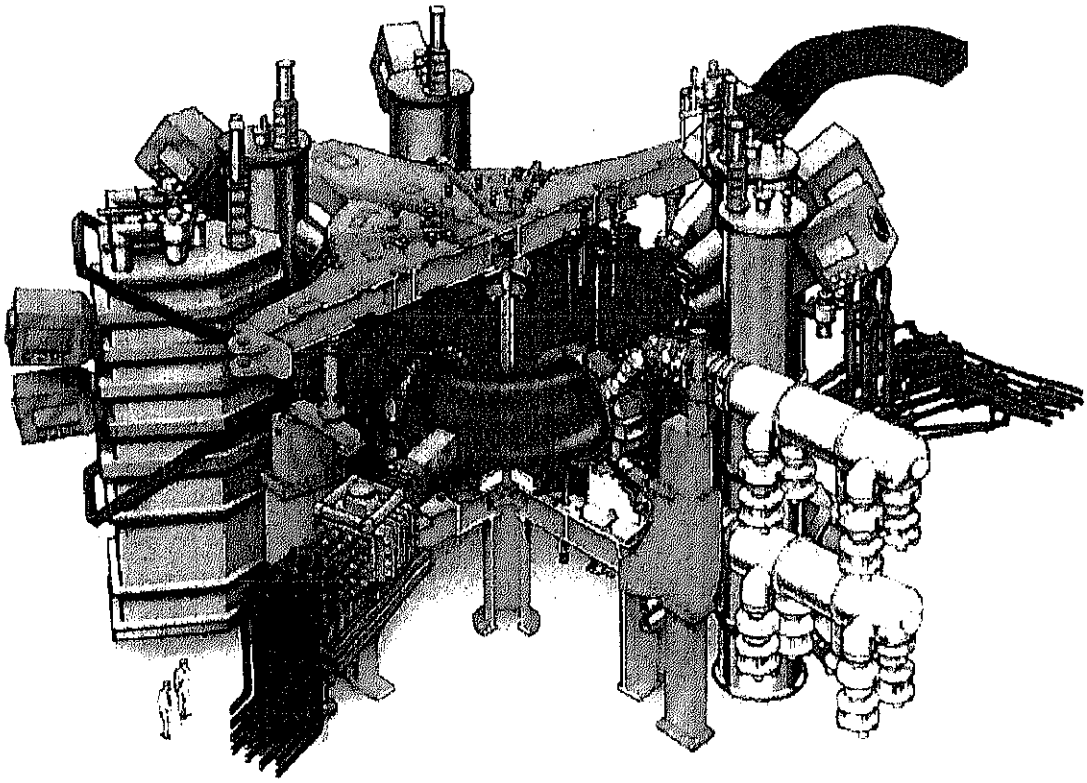

Figure 2.5 *An over schematic of the JT-60U.*

Toroidal magnetic filed B_Φ	: ≦ 4.2 T
Plasma major radius R_0	: 3.0 ~ 3.4 m
Plasma minor radius a: horizontal	0.6 ~1.1 m
b: vertical;	1.0 ~1.7 m
Elongation b/a	: 1.4 ~ 1.7
Plasma current I_p	: ≦ 3 MA
P-NBI P_{NB}	: ~ 28MW (11 units)
N-NBI P_{NNB}	: ~ 10 MW (1 unit)
ICRF P_{IC}	: ~ 5.5 MW
LHCD P_{LH}	: ~ 7 MW
Plasma volume V_p	: ~85m3
Gas puff port	: 6 (4:main, 2:divertor)
Divertor pumping	: 3 ports, 25 m3/s each
Helium pumping	: Argon frosting possible

Table 2.1 *Main parameters of JT-60U.*

systems, one is a positive-ion based NBI (P-NBI) [13] and the other is a negative-ion based NBI (N-NBI) [14].

The P-NBI for the JT-60U started in 1986 with hydrogen beam. All the original neutral beam lines were perpendicular injection. In 1990-1991 four beam-lines out of 14 were modified from perpendicular to tangential injection. At the same time, modification was made to enable deuterium beam operation. By this modification, the highest injection power of positive-ion based NBI system achieved 40MW with deuterium beam from 20 MW with hydrogen beam. The duration of beam injection is up to 10s.

The N-NBI system, which is aiming at 10MW at 500 keV, is composed of one beam-line with two ions sources and a set of high voltage power supply. The beam line is tangential injection, high energy N-NB is effective current drive as well as plasma heating. NNBI also can do the considerably contribute for the fast ion study on JT-60U. In TAE study, until now the experiment was completed only in limited parameter (~ low magnetic filed) by the restriction of Alfven velocity in about 100keV P-NB heated plasma. However, high energy N-NB is enable us to the investigation of the excitation mechanism of TAE instability and transport of the fast ion by TAE near the birth domain of alpha particles in ITER.

In 2002 long beam injection of 10s and high power of 2.6 MW at 360 keV were achieved

2.3.2 Radio frequency heating system

In radio frequency heating, high power electromagnetic waves are injected into the plasma and heat the plasma by resonant interactions. Two main schemes are currently exploited in JT-60U: one is ion cyclotron frequency or its harmonics [15], 110-130 MHz, $2\Omega_{CH}$=116 MHz at Bt=3.8T) and the other is lower-hybrid heating (LHRF at 1.74-2.23 GHz) [16]. Lower-hybrid waves undergo Landau damping by electrons or ions. The design pulse length of these system is 10s. the heating has the advantage of flexible control of the heating profile, since the cyclotron absorption occurs locally. Radio-

frequency waves can be also used for the current drive.

2.3.3 Electron cyclotron heating system

Electron Cyclotron Heating (ECH) systems were installed in 1999, which is an effective tool for the current profile control by local heating and current drive and the MHD instability suppression [17]. The specifications: number of gyrotron is 4, the frequency is 110 GHz, the maximum input power is 1MW and its maximum duration time is 5sec. The absorption width of the wave is 0.1 m.

In 2002 high power of 0.84 MW and long pulse injection for 5s per unit were achieved. Also total injected power of 3 MW was maintained for 2.7 s, which achievement allows the world highest level central electron temperature of about 26 keV for a reversed shear plasma.

2.4 Achievement of JT-60U

JT-60U has achieved high-performance plasmas in various operational modes such as hot ion high confinement mode (H-mode) [18], high-poloidal beta (β_p) H-mode [19, 20], reversed shear (RS) mode [21] and so forth, and contributed in many aspects of ITER physics R&D. Beta is the ratio of the plasma pressure to magnetic field pressure, and reversed shear operation is characterized by a region where the magnetic shear, $s=(r/q)dq/dr$, is negative in the core region.

In 1996 equivalent fusion multiplication factor, $Q_{DT}{}^{eq}=1.05$ was demonstrated in the reverse shear plasma, furthermore in 1998 the record value of equivalent fusion multiplication factor, $Q_{DT}{}^{eq}=1.25$, has been achieved in a deuterium discharge with B_t=4.4T, I_p=2.6MA and q_{95}=3.2 in JT-60U. The neutron emission rate was 3.6×10^{16} s^{-1} with neutral beam power of 12MW [22]. These fusion performance are shown in Lawson diagram as shown in Figure 2.6.

The remarkable progress in the reversed shear operation was demonstrated by its long time sustainment with ELMy H-mode edge. By using power step-down technique,

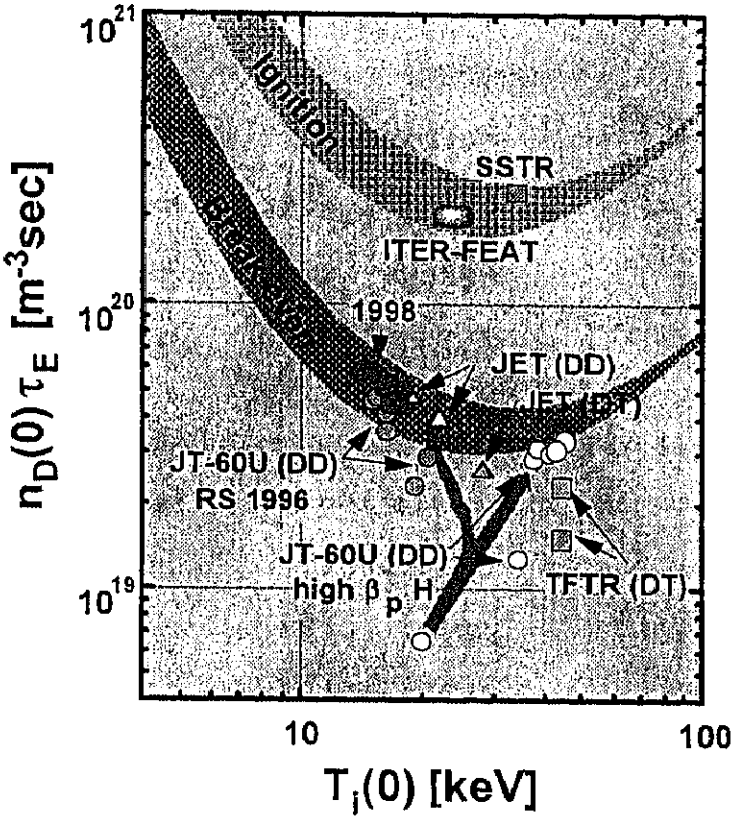

Figure 2.6 *Lawson diagram of JT-60U and other machine experiments.* $Q_{DT}^{eq} = 1.25$ *was achieved in JT-60U reversed shear plasma in 1998.*

the β-collapses were avoided and a favorable performance with H-factor =1.8-2.5 and β_N=1.5-1.8 was sustained for 1.5s [23], where $\beta_N = \beta\,(I_p / aB)^{-1}$ is normalized beta.

In 1999, in a reversed shear plasma fully non-inductive driven current was sustained for 2.6s, where the 70~80% of plasma current I_p was driven by bootstrap current (the current which flows by the plasma pressure gradient) I_{bs} and 20~30% by injected neutral beams I_{NBCD}. The sustained duration was enough for the proof of principle since it was sufficiently longer than the energy confinement than and was comparable to the characteristic relaxation time of the hollow current profile. In which the confinement improvement factor to the ELMy H-mode (H_H-factor) was doubled ($H_H \geqq 2$). Consequently, both bootstrap current fraction I_{bs}/I_p and H_H factor substantially exceed the requirements for the steady operation in ITER (for ITER, $I_{bs}/I_p \sim 50\%$, H_H =1). [24]

In the experimental research in JT-60U on the reversed shear plasmas, a plasma with a 'current hall', a zero-current region at the core part of the toroidal plasma, was discovered. In 2001 experiment, it was confirmed that the current hole was extended up to 40 % of plasma radius and was stably existed for 5s. The ion temperature and the electron density inside the current hall were ~10 keV and ~4×10^{19} m^{-3}, respectively [25]. Though the current hole is an unexpected discovery, this gives many possibility in the future.

2.5 Diagnostics

In order to understand the physical process occurring in a plasma, the JT-60U tokamak is equipped with a comprehensive range of diagnostics system. These measurements can be used to determine the general plasma parameters, assess the fusion performance and for the study of specific plasma phenomena, in order to understand what is happening in a plasma. The parameters most commonly monitored are plasma energy, power input and output, temperature and density profile of electrons and ions, magnetic field configuration and current profile, impurity emission intensity, divertor and edge plasma parameters. Diagnostic tools equipped in JT-60U are summarized in table 2.2

In this study, in order to compare the measured neutron data with a simulated data and to investigate the behavior of fast ions, several diagnostics tools are very important. Here, the important diagnostics in this thesis are explained in detail: Electron temperature profile ($T_e(r)$) and electron density profile ($n_e(r)$), which are measured by Thomson scattering [26]: ion temperature profile ($T_i(r)$) measured by charge exchange recombination spectroscopy [27]: effective charge (Z_{eff}) measured by Bremsstrahung [28].

2.5.1 Thomson scattering

Electron temperature and electron density are simultaneously measured by Thomson

scattering diagnostics with ruby and YAG lasers. In the ruby laser Thomson scattering system, two ruby lasers are used, the wave length, the typical energy and the repetition rate are 694.3 nm (visible), 10J, 0.25Hz, respectively. Two kinds of collection optics provide 60 spatial points: a double Gaussian lens looking at the edge plasma with spatial resolution of 8 mm (20 spatial points) and 16 mm (10 points), and Cassegranian type mirrors viewing core plasma with a spatial resolution of 22 mm (30 points). A scattered light is analyzed by Littrow type spectrometers with 144 photomultiplier tubes and photodiode array.

The ruby Thomson system is not suitable for measuring the time dependent phenomena such as the formation process of an internal transport barrier, since ruby lasers fire at intervals of 4s for each laser. Therefore, a YAG laser Thomson scattering was developed in addition to the ruby Thomson system. The laser wavelength, the energy and the repetition rate are 1064 nm (near infrared), 4J, 50Hz, respectively. For the core plasma measurement, the common collection optics is used, and provide 8 spatial points (spatial resolution of 22mm). Cassegranian type mirrors looking at the edge plasma with spatial resolution of ~30 mm (6 spatial points) . Six channels filter polychromators with silicon Avalanche photodiode detectors are used for one spatial channel.

2.5.2 Charge exchange recombination spectroscopy

In recent years, charge exchange recombination spectroscopy (CXRS) bas become the standard diagnostic for measuring ion temperature profiles on large tokamaks. The method is based on recording the radiation produced when injected atoms perform charge-exchanged with plasma. Neutral atom (D^0) and impurity ion (C^q+) undergo a charge transfer that leaves the product ion in an excited state.

$$D^0 + C^{q+} \rightarrow D^+ + \left[C^{q-1+}\right]^*$$

In usual JT-60U discharges, the source of neutral atom is a neutral beam for plasma heating, and the reaction with C^{6+} is used for this measurement. This is because carbon is a dominant impurity and they are fully stripped throughout the plasma volume.

Main plasma

Plasma parameter	Diagnostics
Ion Temperature Ion density	Charge Exchange Recombination Spectroscopy
Electron Density	Thomson Scattering for Ruby Laser, Thomson Scattering for YAG Laser, CO2 Laser Interferometer, FIR Laser Interferometer U1, U2
Electron Temperature	Thomson Scattering for Ruby Laser , Thomson Scattering for YAG Laser, Electron Cyclotron Emission Diagnostic System
Plasma Current Profile	Motional Stark Effect (MSE)
Radiation	Bolometer
Impurity	VUV Spectrometer for main plasma, Grazing Incident Monochrometer, X-ray Crystal Spectrometer
Z_{eff} (Effective charge)	Z_{eff} (vertical Bremsstrahlung), Tangential Fiber Array for Z_{eff}
Magnetic Fluctuation	Saddle Coil, Tangential Probes for MHD analysis

Scrape off Layer (SOL) and Divertor Plasma

Plasma parameter	Diagnostics
Ion Temperature	VUV Doppler Broadening
Electron Density	Interferometer in Divertor Region, Reciprocating Probe in Divertor Region, Target Langmuir Probe Array
Electron Temperature	Reciprocating Probe in Divertor Region, Target Langmuir Probe Array
Impurity	High Resolution Visible Spectrometer for Divertor, Visible Spectrometer for Divertor, VUV Spectrometer for Divertor Plasma, 60ch Fiber Optics for Divertor, 2D measurement of D-alpha/H-alpha & Impurity emission , Laser Blow-off System
Radiation	Bolometer
Particle Recycling	D-alpha/H-alpha Emission
Neutral Gas Pressure	Neutral Gas Pressure Gauge, Fast Ionization Gauge
Heat Load On Divetor Plate	Infrared TV for Divertor Plate, Divertor Thermocouple (T/C)

Table 2.2 *Summary of JT-60U main diagnostics systems.*

One of heating beams, NB #14 (perpendicular beam), is used for this measurement. Due to above reaction, carbon ions near the neutral beam emit green light (529.2 nm at n=9-7 transition). The light is collected by a quartz lens onto fiber optics and is transmitted to spectrometers in the diagnostic room. The spectrum is detected by intensified CCD cameras for the subsequent analysis of Doppler broadening.

However, according to the ionization balance, there are C^{5+} ions in the edge region, which can emit at the same transition due to direct excitation by electron. Therefore it is important to separate the spectrum by beam excitation from that by electron excitation. In order to subtract the electron excitation light at the edge, CXRS system in JT-60U has an optics for the background spectrum. The number of channel is 36. Spatial and time resolution are 5cm and 16.7 ms, respectively.

2.5.3 Bremsstrahung

In JT-60U, in order to determine Z_{eff} intensity of visible bremsstrahlung is used and light collected by a lens is transmitted by optical fibers from the torus hall to a diagnostic room. Then, the light from the optical fibers passes an interference filter and is detected with a photomultiplier. After the measured intensity is Abel inverted by using SLICE code[ZZ]. After that Z_{eff} can be evaluated by the following relation,

$$Z_{eff} = I_{brem} \Big/ \left[7.58 \times 10^{-21} \frac{\Delta\lambda}{\lambda} g(T_e) \frac{n_e^2 \exp(-12400.0 / \lambda T_e)}{\sqrt{T_e}} \right]$$

where I_{brem} is the Abel inverted intensity of Bremsstrahung, $g(T_e)$ is the Gaunt factor, and λ=52326.2 Å, $\Delta\lambda$ =10.0 Å and T_e is in eV. In addition, the electron temperature and density must also be known.

References

[1] N. Peacock, et al. Nature **224** (1969) 448

[2] R. Herman, Fusion: The Search for Endless Energy, Cambridge University Press 1991

[3] J. Wesson, Oxford Engineering Science Series 48 Tokamaks second edition, Oxford University press, 1997

[4] JET Team, Nucl. Fusion **32** (1992) 187

[5] S. Ishida, et al., Phys. Rev. Lett. **79** (1997) 3917

[6] The JET Team, in 17th International Conference on Plasma Physics and Controlled Nuclear Fusion Research, IAEA Yokohama 1998.

[7] R. J. Hawryluk and TFTR Team, in 15th International Conference on Plasma Physics and Controlled Nuclear Fusion Research, <IAEA-CN-60/A-1-I-1>

[8] F. Wagner, et al., Phys. Rev. Lett. **49** (1982) 1408

[9] T. Fujita, et al., Phys. Rev. Lett. **78** (1997) 2337

[10] H. Ninomiya, et al., Plasma Devices Operat. **1** (1990) 43

[11] Y. Koide and the JT-60 Team, Phys. Plasma **4** (1997) 1623

[12] H. Hosogane, et al., Proc, 16th Int. Conf. Montreal, 3 (IAEA. Vienna, 1969) 555

[13] M.Kuriyama et al. Fusion Science and Technology **42** (2002) 410

[14] M.Kuriyama et al. Fusion Science and Technology **42** (2002) 424

[15] S. Moriyama, et al. Fusion Science and Technology **42** (2002) 467

[16] M. Seki, et al., Fusion Science and Technology **42** (2002) 452

[17] Y. Ikeda, et al., Fusion Eng. and Design, **53** (2001) 351

[18] H. Shirai, T. Takizuka, M. Sato, et al., "Analyses of Electron and Ion Transport Properties in JT-60U H-mode Plasmas with Improved Core Confinement", proc. 23rd EPS Conf., Kiev, Part I (1996) 339.

[19] Y. Kamada, , et al., Plasma Phys. Cont. Nucl. Fusion Res. Proc.15th Int. Conf.

(Seville, 1994) Vol 1, p651.

[20] Y. Kamada, et al., Fusion Energy Proc. 16th Int. Conf. (Montreal, 1996) Vol **1**, p247.

[21] T. Ozeki, M. Azumi, T. Tsunematsu et al., in Proc. of the 14th Int. Conf. on Plasma Physics and Controlled Nucl. Fusion Research, Wuzburg, 1992 (IAEA, Vienna), Vol.**2**, 187 (1993).

[22] T. Fujita, et al., Proc. of 17th International Conference on Plasma Physics and Controlled Nuclear Fusion Research, IAEA Yokohama 1998 (IAEA. Vienna) <IAEA-CN-69/EX1/2>

[23] Y. Kamada, et al., proc. of 17th International Conference on Plasma Physics and Controlled Nuclear Fusion Research, IAEA Yokohama 1998 (IAEA. Vienna) <IAEA-CN-69/EX9/2>

[24] S. Ide, et al., Nucl. Fusion, **40** (2000) 445

[25] T. Fujita, et al., Phys. Rev. Lett., **87** (2001) 245

[26] T. Hatae, et al., Rev. Sci. Instrum. **70** (1999) 772

[27] Y. Koide, et al., Rev. Sci. Instrum. **72** (2001) 119

[28] K Kadota et al., Nucl. Fusion **20** (1980) 209